THE JOURNAL OF PHYSICAL CHEMISTRY B

pubs.acs.org/JPCB Article

Strong Concentration Enhancement of Molecules at the Interface of Aqueous Microdroplets

Published as part of The Journal of Physical Chemistry virtual special issue "W. E. Moerner Festschrift".

Hanqing Xiong, Jae Kyoo Lee, Richard N. Zare,* and Wei Min*

Cite This: *J. Phys. Chem. B* 2020, 124, 9938–9944 Read Online

ACCESS | Metrics & More | Article Recommendations | Supporting Information

ABSTRACT: Water is arguably the most common and yet least understood material on Earth. The interface between water and a hydrophobic medium, such as air, oil, or lipids, plays a fundamental role in chemistry and biology. However, the behavior of molecules at interface of micron-sized water droplets (microdroplets) in such media is poorly characterized. Herein we employed two-photon fluorescence microscopy and Förster resonant energy transfer imaging to study the probe localization in water−oil microdroplets with high contrast and resolution. We found that there exists a general effect of surface enrichment and orientation alignment for water-soluble probes. Remarkably, probes are concentrated into a ∼10 nm thin layer at the microdroplet water−oil interface by up to 10 000-fold compared to the bulk counterpart. We suggest that the strong enrichment and alignment of water-soluble molecules, likely to be induced in part by a local electric field at the interface, could be a major factor accounting for orders of magnitude faster reaction rates observed in aqueous microdroplets compared to their bulk counterparts.

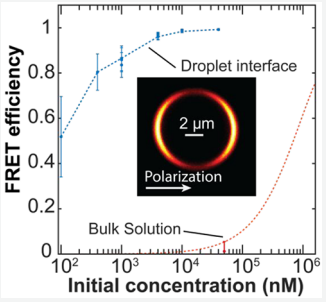

INTRODUCTION

Microdroplet chemistry has recently emerged as a unique platform, as reactions in liquid microdroplets often exhibit unusual kinetic and thermodynamic properties that are not observed in bulk solution.[1−13] Remarkably, reaction rates can be accelerated by factors of 10^3 or more in microdroplets compared to bulk solution. Among the possible underlying mechanisms, the enrichment at the interface of microdroplets has been considered as a potential factor.[6] Indeed, it was reported long ago that the adsorption of some organic dyes at the water−oil interface was observed with fluorescence polarization anisotropy.[14,15]

In the context of water microdroplets, it has been recently reported using confocal microscopy that rhodamine 6G, a positively charged dye, exhibits strong fluorescence polarization anisotropy at the water−oil interface of microdroplets and higher fluorescence intensity at the interface (by a factor of 5−10) than in the interior.[16] These earlier observations motivated us to systematically investigate the spatial distribution of various molecules in microdroplets made of different solvents under rigorous experimental conditions. In what follows, we employ advanced optical microscopy to reveal the probe localization with high imaging contrast and spatial resolution. The results in this study shed light on understanding why the rates of many reactions in water microdroplets are markedly accelerated compared to the rates of the same reactions in bulk water.

METHODS

To keep the main text concise, the methods employed and materials used are presented at length in the Supporting Information.

RESULTS

Surface Enrichment Effect Studied by Two-Photon Fluorescence Imaging. Microdroplets are placed onto superhydrophobic coverslips after being prepared by ultrasonic emulsification and sealed in closed microchambers (see Materials and Methods in the Supporting Information and Figure 1a,b) to minimize the perturbation to the water−oil interface. We employed a home-built two-photon excited fluorescence microscope equipped with a single-photon counting module (see Materials and Methods and Figure 1c−e and Figure S1). The two-photon fluorescence excitation intrinsically has a neglectable out-of-focus background compared to one-photon confocal excitation.[17] In addition, the low dark counts single-photon counting module has noise reduction superior to that of an analog detection circuit of a photomultiplier tube used in a typical confocal microscope. These advantages result in a much higher dynamic range of our

Received: August 24, 2020
Revised: October 8, 2020
Published: October 21, 2020

https://dx.doi.org/10.1021/acs.jpcb.0c07718
J. Phys. Chem. B 2020, 124, 9938–9944

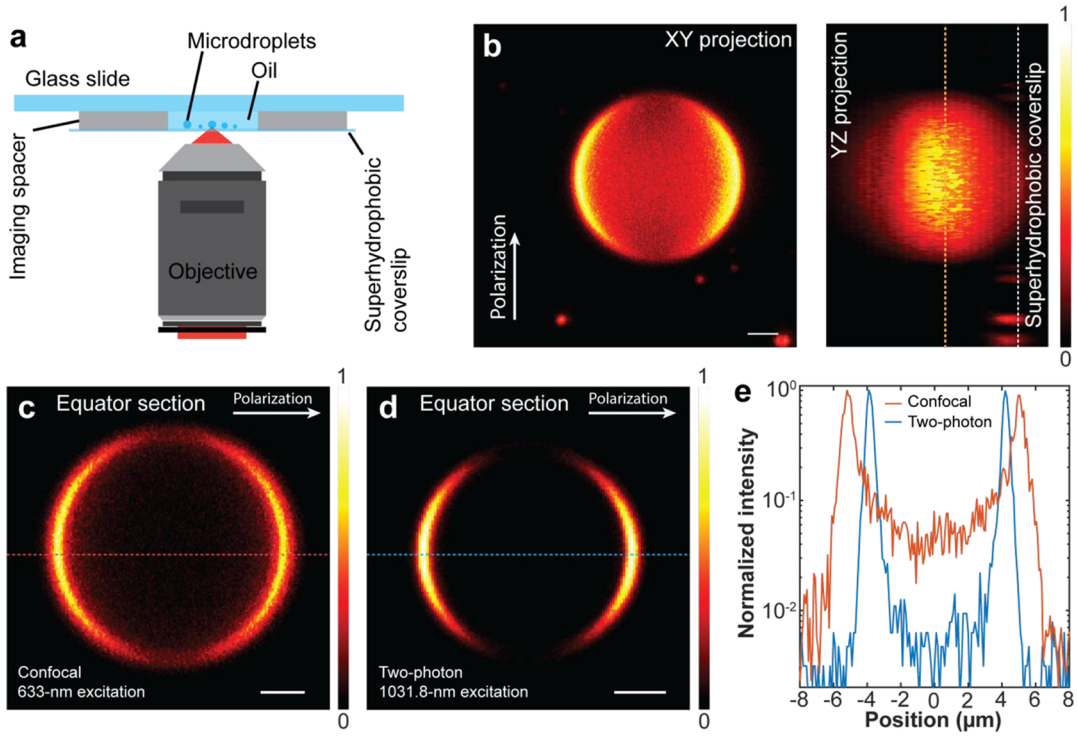

Figure 1. Sample preparation and system optimization of fluorescence imaging of water microdroplets in oil. (a) Schematic of the experimental setup. (b) Typical three-dimensional confocal imaging of a microdroplet in hexadecane. The droplet is prepared using a 20 μM Alexa 633 aqueous solution surrounded by hexadecane. The maximum intensity projections on *XY* and *YZ* planes show that the contact between the droplet and the surface of the superhydrophobic coverslip (white dashed line) makes a negligible contribution to the image. (c) Corresponding confocal imaging of the equator plane (labeled on (b) by an orange dashed line). (d) Typical image of the equator planes of microdroplets on the same sample (not the same droplet) using our home-built two-photon fluorescence microscope equipped with single-photon counting. (e) Normalized fluorescence intensity distributions along the red and blue dashed lines labeled on (c) and (d), respectively. In (b)−(d), the white arrows show the polarization of the excitation field. Scale bar: 2 μm.

home-built system. With these optimizations, the intensity of interface fluorescence reached ~200 times more than that of the interior, which is more than 10-times larger than that of the image acquired by single-photon confocal microscopy (Figure 1c−e).

Our probe dependence study indicates that there exists a general surface enrichment effect for water-soluble molecules, including negatively charged Alexa 633 and Alexa 647 (Figure 2a, Figure S2a), neutral zwitterion rhodamine 101 (Figure 2b), and positively charged rhodamine 6G, ATTO Rho14, and rhodamine 800 (Figure 2c, Figure S2b,c). Moreover, all the interface signals show strong anisotropy corresponding to the excitation polarization (Figure 2a−c, Figure S2), suggesting probe alignment with a preferred dipole orientation.[18] This observed fluorescence polarization anisotropy at the microdroplet interface is consistent with the findings reported in a previous study.[16] Again, the intensity of interface fluorescence can reach 100 times more than that of the interior (Figure 2d). This ratio is much more pronounced than the earlier report (only 5−10) by using a confocal setup,[16] caused by the lower out-of-focus background and higher dynamic range offered by our two-photon microscope. We also note that the surface enrichment effect is saturable, as the optical contrast between the interface and the interior diminishes when the probe concentration increases (Figure S3).

Further study on solvent dependence suggests that this effect is unique to water. When microdroplets are prepared from other polar organic solvents (such as protic methanol and aprotic DMSO) in the same oil medium (Figures 2e,f), the probe intensity distributions become homogeneous and isotropic. This observation suggests that there exist mechanisms other than the potential hydrophobic interaction (if any) between the dyes and the oil surface. Further support is provided by the chemical nature of Alexa 633 and Alexa 647 with multiple sulfonate groups that are highly hydrophilic.

In addition to the solvent dependence, another interesting phenomenon of the enriched molecules is the abnormal dimerization equilibrium (Figure 3). It is well-known that some cationic dyes tend to form dimers in aqueous solution. For example, Sekiguchi and co-workers[19] have shown that rhodamine 800 (Rh800) molecules tend to form so-called H-dimers (Figure 3a) in bulk water solution with an equilibrium constant K_{eq} = 2.8 × 10^4 mol^{-1} dm^3. This dimer formation induces a change in the concentration-dependent absorption spectrum at room temperature. The absorption of the H-dimer is blue-shifted when compared with that of the monomer. Consequently, a shoulder peak around 630 nm rises as the concentration of Rh800 in bulk water increases (dashed curves in Figure 3b). Different from the behavior in bulk water solution, the Rh800 absorption spectra measured at the water−oil interface are always the same as the monomer absorption spectrum reported by Sekiguchi et al. (solid curves in Figure 3b), though the concentrations of Rh800 at the interface are greatly enhanced when compared with the corresponding cases in bulk solution (Figure S2C). This result indicates that the Rh800 is predominately in the monomer form at the microdroplet interface.

https://dx.doi.org/10.1021/acs.jpcb.0c07718
J. Phys. Chem. B 2020, 124, 9938−9944

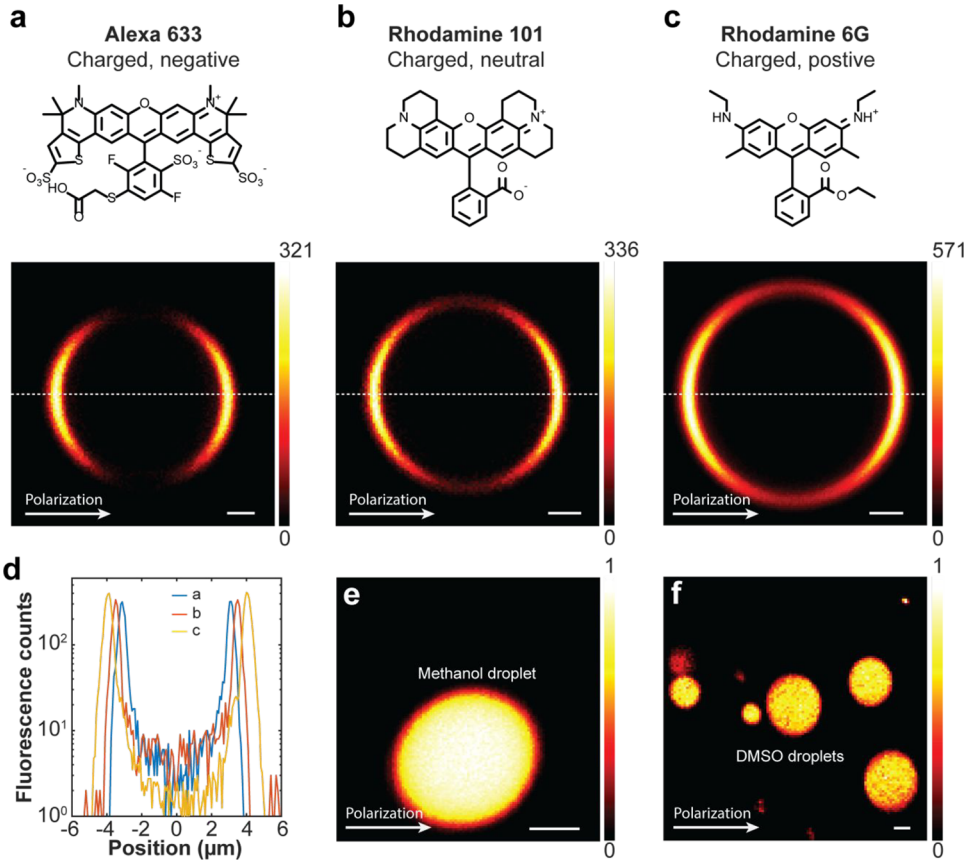

Figure 2. Enrichment of charged dye molecules at the water−oil interface of aqueous microdroplets. (a)−(c) Typical two-photon fluorescence images of aqueous droplets with negatively charged dye Alexa 633, neutral zwitterion rhodamine 101 inner salt, and positively charged dye rhodamine 6G, respectively. All microdroplets are prepared by sonicating the corresponding 40 μM dye aqueous solutions in hexadecane. (d) Distribution of fluorescence counts along the dashed white lines labeled in (a)−(c), respectively. (e) and (f) Two-photon fluorescence images of microdroplets prepared by 40 μM rhodamine 6G dissolved in methanol and dimethyl sulfoxide (DMSO) distributed in hexadecane, respectively. Different from (a)−(c) (in which the droplets stand on superhydrophobic coverslip), the droplets in (e) and (f) were imaged when they were still suspended and moving in hexadecane, and the distortion of the droplets is caused by the slight motion during image scanning. White arrows show the polarization of the laser excitation field. The color bars of (a)−(c) represent photon counts within 0.4 ms; the color bars of (e) and (f) represent the normalized intensity. Scale bars: (a)−(c), 1 μm; (e) and (f), 2 μm.

High-Resolution Imaging of Probe Localization by FRET. We note that the full width at half-maximum (fwhm) of the interface mapped out by two-photon fluorescence imaging is ∼400 nm (Figure 2), which is quite close to the diffraction-limited theoretical fwhm[17] (∼320 nm) of our system. When optical aberrations are taken into consideration, the dye layer would be much thinner than our resolution, suggesting even higher local enrichment than the measured apparent factor of ∼200. To determine the true probe location, we employed Förster resonant energy transfer (FRET)[20,21] microscopy, which provides a powerful means for measuring the distance between probe molecules with a nm-level resolution.

Figure 4a shows the spectral configuration of our FRET experiment. Two positively charged probes, ATTO Rho14 and rhodamine 800 (Rh800), each becoming enriched at the microdroplet surface when acting alone (Figure S2b,c), were selected as the donor/acceptor pair, as the emission of ATTO Rho14 well overlaps with the absorption of Rh800. Two-photon excitations at two different wavelengths were performed separately. Excitation at 860 nm can only be absorbed by the donor (Table S1), allowing us to estimate the FRET efficiency with known donor and acceptor quantum yields (80% for ATTO Rho14 and 3.8% for Rh800[22] in water) (details in the Materials and Methods). Excitation at 1031.8 nm can be absorbed by both the donor and the acceptor efficiently, which is used to estimate the number of acceptor molecules in the excitation volume (details in the Materials and Methods).

In one typical example, microdroplets were prepared with merely 4 μM FRET pair solution. Although the quantum yield of the acceptor is much lower than that of the donor (i.e., 3.8% for Rh800[22] and 80% for ATTO Rho14 in water), an signal in the acceptor channel (Figure 4c) even higher than that in the donor channel (Figure 4b) is observed under 860 nm excitation, suggesting that the FRET process between this pair is highly efficient. As a comparison, the acceptor channel is undetectable in bulk water solution with even a much higher concentration of the FRET pair at 50 μM (Table S2). Quantitatively, the FRET efficiency is determined to be 97 ± 1% at the interface (Figure 4f, Materials and Methods). Excitation at 1031.8 nm (Figure 4d,e) provides an easy way to estimate the number of acceptor molecules (N) in the excitation volume, by comparing the fluorescence intensities from the *direct* acceptor excitation at the water−oil interface with the reference intensity measured in 50 μM bulk solution (dashed line in Figure 4g, Table S1, and Materials and Methods). Similar to this example prepared at 4 μM, 10 independent measurements were performed for droplets at

https://dx.doi.org/10.1021/acs.jpcb.0c07718
J. Phys. Chem. B 2020, 124, 9938−9944

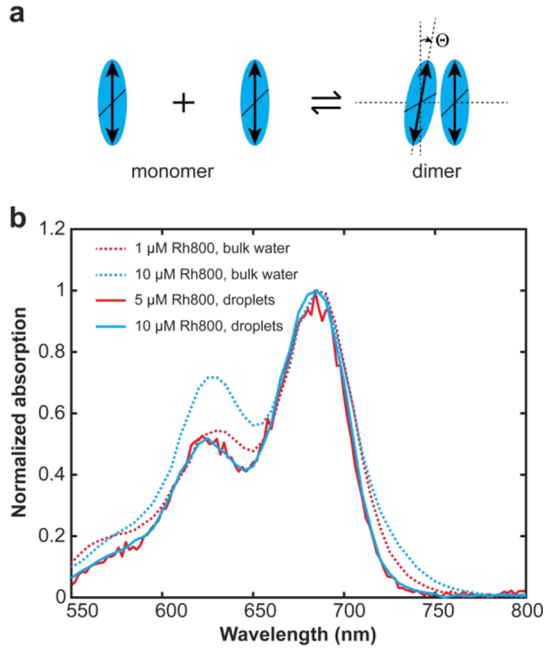

Figure 3. Abnormal dimerization equilibrium of rhodamine 800 (Rh800) at the water−oil interface of aqueous microdroplets. (a) Diagram of dimerization equilibrium for dye molecules that form an H-dimer. The arrows show the axes of transition dipole moments. Θ represents a possible twisted angle. (b) Absorption spectra of Rh800 measured in 1 μM bulk water solution (red dashed curve) and 10 μM bulk water solution (blue dashed curve), and at the water microdroplet interfaces prepared by 5 μM water solution (red curve) and 10 μM water solution (blue curve) in hexadecane, respectively. The measurement details can be found in the Materials and Methods.

different initial concentrations (from 100 nM to 10 μM, Figure S4), with the corresponding FRET efficiency and the number of acceptor molecules determined.

Global analysis of the above experiments yields valuable information about the probe location and allows the estimation of the effective thickness of the dye-enriched layer at the interface. We calculated the effective dye layer thickness at the microdroplet interface by comparing the observed FRET efficiency with the theoretical bulk FRET efficiency assuming that most of the dyes exhibiting FRET are localized in the layer. The classic FRET theory[21,23] for a randomly oriented system predicts the FRET efficiency as a function of acceptor concentration (with minor modification caused by spatial alignment at the interface, details in the Materials and Methods). As shown in Figure 4h, this curve allows us to determine 10 acceptor concentrations $[c]$ at the interface from FRET efficiencies calculated from 10 independent measurements. When plotting these 10 resulting $[c]$ values against the number of molecules (N) in the excitation volume, a strong linear correlation is discovered (Figure 4i). We note a simple relationship exists between $[c]$ and N: $AdN_A[c]=N$. Here $A = 3.2 \times 10^5$ nm^2 is the axial focal area of our microscope (details in the Materials and Methods), d is the effective dye layer thickness, and N_A is the Avogadro number. Thus, the observed linear correlation between $[c]$ and N suggests that d would be independent of probe concentration, and it should reflect the intrinsic range of the driving force at the interface. A linear regression gives an average $d = 10 \pm 1$ nm (Figure 4i), which is indeed much thinner than the diffraction limit.

DISCUSSION AND CONCLUSIONS

Quantification of the enrichment phenomenon is possible with the FRET imaging measurements. Figure 4j summarizes the FRET efficiencies measured on microdroplets prepared by different initial acceptor concentrations. Meanwhile, the theoretical FRET efficiencies from a random system (i.e., bulk solution) are also plotted for comparison: drastically different concentrations are needed to achieve the same FRET efficiency. For example, droplets prepared with 100-nM FRET pairs could result in a FRET efficiency up to 0.51 ± 0.17, which can only be achieved in bulk solution with millimolar-level concentrations (dashed curve, Figure 4j). Therefore, in the relatively low concentration range, the confinement of dye molecules into a ∼10 nm thin layer can enrich the local probe concentration by approximately 10 000 times. This result has important implications for accelerating reaction kinetics.

The observations of the enrichment of molecules with different charges and molecular structures on the water−oil interface suggest that the enrichment effect might be a relatively general phenomenon. It is possible for the residual hydrophobic interactions between the dye molecules and the water/oil interface to make some contribution to this enrichment effect. Yet, we have experimental evidence that suggests that this cannot be the main mechanism. On the one hand, the enrichment effect is unique to water (Figure 2), which indicates that the attraction of dye molecules to oil (if any) cannot be the main explanation for this behavior. Otherwise, one would have observed the same dye enrichment for microdroplets prepared from methanol or DMSO in the same oil medium. On the other hand, recall that the sulfonated dyes are highly soluble in water (i.e., little exclusion from water) but still show this marked concentration at the periphery of the water microdroplet suggests that the enrichment effect can still occur without involving the exclusion from water. Taken together, these experiments suggest that hydrophobic interactions (attraction to oil and/or exclusion by water) cannot be the main driving force.

Among other possible mechanisms, we speculate the electric field formed at the microdroplet water−oil interface might play an important role. We recently determined that water microdroplets in hexadecane oil show an electric field of about 10^7 V/cm at the interface.[24] This strong field likely arises from charge separation caused by the adsorption of negative ions at the water−oil interface of microdroplets. The field gradient in the diffusion layer of the double-layer structure may serve as a driving force to concentrate molecules with charges or large dipole moments at the water−oil interface. This electric field also provides a natural explanation for the orientation alignment of molecules at the interface. Furthermore, the abnormal dimerization equilibrium of Rh800 at the interface (Figure 3) also appears to support the electric field effect. Dimerization requires a specified orientation between the two monomers in most cases (such as a twisted angle between the transition dipole moments[25] (Figure 3a)). Therefore, dimerization is not favored in a strong electric field because the dipoles of the molecules become rigidly aligned by the field and a specific dimerization geometry has to overcome a potential barrier.

It has been well documented that many reactions involving charged or polar species can be accelerated by a factor of 10^3 or more inside microdroplets.[1−13] Indeed, the rates of acid-catalyzed or base-catalyzed reactions are markedly enhanced in

https://dx.doi.org/10.1021/acs.jpcb.0c07718
J. Phys. Chem. B 2020, 124, 9938−9944

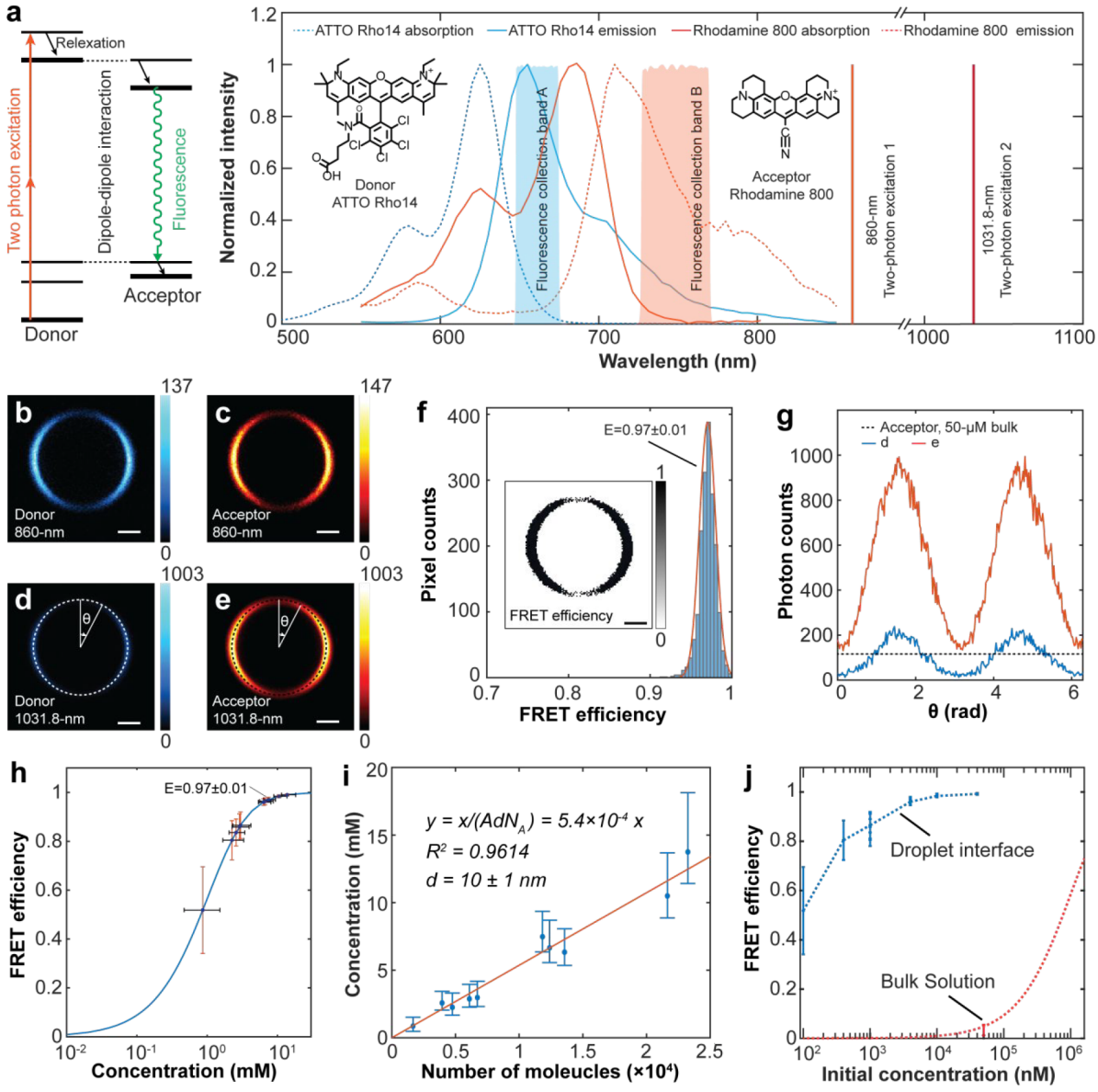

Figure 4. Förster resonant energy transfer (FRET) imaging of the water−oil interface of microdroplets in hexadecane. (a) Energy diagram and spectral configuration of two-photon excited FRET. Blue (dashed and solid) and red (solid and dashed) curves show the absorption and emission spectra of the donor (ATTO Rho14) and acceptor (rhodamine 800), respectively. Excitation at 860 nm can only be absorbed by the donor, whereas excitation at 1031.8 nm can be absorbed efficiently by both the donor and the acceptor. Blue and red bands show the two fluorescence collection channels. (b) and (c) Unmixed fluorescence signals from two-photon excitation at 860 nm (details in the Materials and Methods) of the donor and acceptor from the same microdroplet (prepared by 4 μM donor and 4 μM acceptor water solution in hexadecane), respectively. (d) and (e) Unmixed fluorescence signals from two-photon excitation at 1031.8 nm of the donor and acceptor from the same microdroplet, respectively. From (b) and (c), the FRET efficiency distribution was calculated (inset in (f)). (f) Histogram of FRET efficiency (the inset). In (f), FRET efficiencies of pixels with donor intensity less than 16 counts are not considered because of the shot noise. (g) Radical distributions of fluorescence photon counts of the donor (b) and the acceptor (c) as the angle in (d) and (e). The dashed line shows the fluorescence intensity measured at the same condition in 50 μM acceptor in bulk water as a reference. (h) FRET efficiency as a function of acceptor concentration. The blue curve is the theoretical calculation for FRET pairs with parallel transition-dipole orientations (details in the Materials and Methods), which is used to find the real concentrations of FRET measurements (dots) by a look-up-table manner, respectively. The point for the measurement $E = 0.97 \pm 0.01$ is indicated. (i) Concentration as a function of the number of molecules in the excitation volume. (j) FRET efficiencies at the water−oil interface of microdroplets prepared at different initial concentrations of the acceptor. The theoretical FRET efficiency of the bulk solution (i.e., random system) is plotted as a reference (with one measurement at 50 μM indicated). The color bar represents fluorescence counts in a 0.4 ms dwell time. Scale bar: 2 μm.

water microdroplets.[3,8] Because of the large surface-to-volume ratio of microdroplets compared to bulk solution, it is expected that reactions at or near the interface become dominant in accounting for the difference. It has been recently suggested that solvation energy differences between bulk and interface play a key role in the rate constant increase.[26] A major unanswered question is to what extent reactants are concentrated at or near the interface in the context of water

https://dx.doi.org/10.1021/acs.jpcb.0c07718
J. Phys. Chem. B 2020, 124, 9938−9944

microdroplets. Our observed enrichment of molecules to the ~10 nm thin layer by up to 10 000 times could significantly increase collision frequencies, which might be one of the main mechanisms for rate accelerations. This concentration effect will be especially important for reaction intermediates that exist in low concentrations (Figure 4j). As the bulk reactant concentration increases, the number of reactant molecules residing in this thin layer becomes saturated (Figure S3), making it less significant compared to that of the bulk interior. This observation is consistent with the saturation effect on the spontaneous reduction in microdroplets.[27] Another possible contributing factor is the orientation alignment of reactants. The tight alignment and confinement of the charged molecules into a two-dimensional thin layer strongly restrict the rotation freedom and one degree of translation freedom. A previous study using fluorescence lifetime imaging microscopy reported that intramolecular rotation of molecular rotors is restricted at the water−oil interface of microdroplet.[28] Such a decrease in system entropy may contribute to the thermodynamic alternation of reactions reported recently.[11,12] The present study concerns water droplets surrounded by a hydrophobic oil medium. We believe that this concentration enrichment phenomenon does apply to any droplet showing an electric double layer, such as a charged droplet consisting primarily of an organic solvent. All these factors may work together to provide the beginning of a comprehensive understanding why microdroplet chemistry differs so markedly compared to bulk solution.

■ ASSOCIATED CONTENT

Supporting Information

The Supporting Information is available free of charge at https://pubs.acs.org/doi/10.1021/acs.jpcb.0c07718.

Materials, methods, and calculations; diagram of imaging system, fluorescence images, FRET measurements and models (Figures S1−S5); fluorescence measurements (Tables S1 and S2) (PDF)

■ AUTHOR INFORMATION

Corresponding Authors

Richard N. Zare − *Department of Chemistry, Stanford University, Stanford, California 94305, United States;* orcid.org/0000-0001-5266-4253; Email: zare@stanford.edu

Wei Min − *Department of Chemistry, Columbia University, New York, New York 10027, United States;* orcid.org/0000-0003-2570-3557; Email: wm2256@columbia.edu

Authors

Hanqing Xiong − *Department of Chemistry, Columbia University, New York, New York 10027, United States*

Jae Kyoo Lee − *Department of Chemistry, Stanford University, Stanford, California 94305, United States;* orcid.org/0000-0002-1257-8737

Complete contact information is available at: https://pubs.acs.org/10.1021/acs.jpcb.0c07718

Notes

The authors declare no competing financial interest.

■ ACKNOWLEDGMENTS

This paper is dedicated to W. E. Moerner, who is a master of molecular microscopy. We thank support from NSF CHE-1904684 (to W.M.) and the Air Force Office of Scientific Research AFOSR FA9550-16-1-0113 (to RNZ).

■ REFERENCES

(1) Lee, J. K.; Kim, S.; Nam, H. G.; Zare, R. N. Microdroplet fusion mass spectrometry for fast reaction kinetics. *Proc. Natl. Acad. Sci. U. S. A.* **2015**, *112* (13), 3898−3903.

(2) Lee, J. K.; Banerjee, S.; Nam, H. G.; Zare, R. N. Acceleration of reaction in charged microdroplets. *Q. Rev. Biophys.* **2015**, *48* (4), 437−444.

(3) Banerjee, S.; Zare, R. N. Syntheses of isoquinoline and substituted quinolines in charged microdroplets. *Angew. Chem., Int. Ed.* **2015**, *54* (49), 14795−14799.

(4) Badu-Tawiah, A. K.; Campbell, D. I.; Cooks, R. G. Accelerated C−N bond formation in dropcast thin films on ambient surfaces. *J. Am. Soc. Mass Spectrom.* **2012**, *23* (9), 1461−1468.

(5) Bain, R. M.; Pulliam, C. J.; Cooks, R. G. Accelerated Hantzsch electrospray synthesis with temporal control of reaction intermediates. *Chemical Science* **2015**, *6* (1), 397−401.

(6) Fallah-Araghi, A.; Meguellati, K.; Baret, J.-C.; Harrak, A. E.; Mangeat, T.; Karplus, M.; Ladame, S.; Marques, C. M.; Griffiths, A. D. Enhanced Chemical Synthesis at Soft Interfaces: A Universal Reaction-Adsorption Mechanism in Microcompartments. *Phys. Rev. Lett.* **2014**, *112* (2), 028301.

(7) Girod, M.; Moyano, E.; Campbell, D. I.; Cooks, R. G. Accelerated bimolecular reactions in microdroplets studied by desorption electrospray ionization mass spectrometry. *Chemical Science* **2011**, *2* (3), 501−510.

(8) Müller, T.; Badu-Tawiah, A.; Cooks, R. G. Accelerated Carbon-Carbon Bond-Forming Reactions in Preparative Electrospray. *Angew. Chem., Int. Ed.* **2012**, *51* (47), 11832−11835.

(9) Lee, J. K.; Nam, H. G.; Zare, R. N. Microdroplet fusion mass spectrometry: Accelerated kinetics of acid-induced chlorophyll demetallation. *Q. Rev. Biophys.* **2017**, *50*, E2.

(10) Jansson, E. T.; Lai, Y.-H.; Santiago, J. G.; Zare, R. N. Rapid hydrogen−deuterium exchange in liquid droplets. *J. Am. Chem. Soc.* **2017**, *139* (20), 6851−6854.

(11) Nam, I.; Nam, H. G.; Zare, R. N. Abiotic synthesis of purine and pyrimidine ribonucleosides in aqueous microdroplets. *Proc. Natl. Acad. Sci. U. S. A.* **2018**, *115* (1), 36−40.

(12) Nam, I.; Lee, J. K.; Nam, H. G.; Zare, R. N. Abiotic production of sugar phosphates and uridine ribonucleoside in aqueous microdroplets. *Proc. Natl. Acad. Sci. U. S. A.* **2017**, *114* (47), 12396−12400.

(13) Wei, Z.; Li, Y.; Cooks, R. G.; Yan, X. Accelerated Reaction Kinetics in Microdroplets: Overview and Recent Developments. *Annu. Rev. Phys. Chem.* **2020**, *71*, 31−51.

(14) Ishizaka, S.; Nakatani, K.; Habuchi, S.; Kitamura, N. Total internal reflection fluorescence dynamic anisotropy of sulforhodamine 101 at a liquid/liquid interface: Rotational reorientation times and interfacial structures. *Anal. Chem.* **1999**, *71* (2), 419−426.

(15) Ishizaka, S.; Kim, H.-B.; Kitamura, N. Time-resolved total internal reflection fluorometry study on polarity at a liquid/liquid interface. *Anal. Chem.* **2001**, *73* (11), 2421−2428.

(16) Zhou, Z.; Yan, X.; Lai, Y.-H.; Zare, R. N. Fluorescence Polarization Anisotropy in Microdroplets. *J. Phys. Chem. Lett.* **2018**, *9* (11), 2928−2932.

(17) Zipfel, W. R.; Williams, R. M.; Webb, W. W. Nonlinear magic: multiphoton microscopy in the biosciences. *Nat. Biotechnol.* **2003**, *21* (11), 1369−1377.

(18) Meath, W. J.; Power, E. On the importance of permanent moments in multiphoton absorption using perturbation theory. *J. Phys. B: At. Mol. Phys.* **1984**, *17* (5), 763−781.

(19) Sekiguchi, K.; Yamaguchi, S.; Tahara, T. Formation and dissociation of rhodamine 800 dimers in water: steady-state and

ultrafast spectroscopic study. *J. Phys. Chem. A* **2006**, *110* (8), 2601−2606.
(20) Fő rster, T. 10th Spiers Memorial Lecture. Transfer mechanisms of electronic excitation. *Discuss. Faraday Soc.* **1959**, *27*, 7−17.
(21) Medintz, I. L.; Hildebrandt, N. *FRET-Förster resonance energy transfer: from theory to applications*; John Wiley & Sons, 2013.
(22) Jin, T. Near-infrared fluorescence detection of acetylcholine in aqueous solution using a complex of rhodamine 800 and p-sulfonatocalix[8]arene. *Sensors* **2010**, *10* (3), 2438−2449.
(23) Förster, T. Experimentelle und theoretische Untersuchung des zwischenmolekularen Übergangs von Elektronenanregungsenergie. *Z. Naturforsch., A: Phys. Sci.* **1949**, *4* (5), 321−327.
(24) Xiong, H.; Lee, J. K.; Zare, R. N.; Min, W. Strong Electric Field Observed at the Interface of Aqueous Microdroplets. *J. Phys. Chem. Lett.* **2020**, *11* (17), 7423−7428.
(25) Terdale, S.; Tantray, A. Spectroscopic study of the dimerization of rhodamine 6G in water and different organic solvents. *J. Mol. Liq.* **2017**, *225*, 662−671.
(26) Narendra, N.; Chen, X.; Wang, J.; Charles, J.; Cooks, R. G.; Kubis, T. Quantum Mechanical Modeling of Reaction Rate Acceleration in Microdroplets. *J. Phys. Chem. A* **2020**, *124*, 4984.
(27) Lee, J. K.; Samanta, D.; Nam, H. G.; Zare, R. N. Micrometer-sized water droplets induce spontaneous reduction. *J. Am. Chem. Soc.* **2019**, *141*, 10585−10589.
(28) Kang, J.; Lhee, S.; Lee, J. K.; Zare, R. N.; Nam, H. G. Restricted Intramolecular Rotation of Fluorescent Molecular Rotors at the Periphery of Aqueous Microdroplets in Oil. *Sci. Rep.* **2020**, *10*, 16859.

https://dx.doi.org/10.1021/acs.jpcb.0c07718
J. Phys. Chem. B 2020, 124, 9938−9944